

P. K.-B. Chao¹

Graduate Student,
Department of Chemical
Engineering,
University of Pennsylvania,
Philadelphia, Pa. 19104

H. Ozoe

Associate Professor,
Department of Industrial and
Mechanical Engineering,
Okayama University,
Okayama, Japan

S. W. Churchill

Carl V. S. Patterson Professor
of Chemical Engineering.

Department of Chemical Engineering,
University of Pennsylvania,
Philadelphia, Pa. 19104

N. Lior

Associate Professor,
Department of Mechanical
Engineering and Applied Mechanics
University of Pennsylvania,
Philadelphia, Pa. 19104
Mem. ASME

Laminar Natural Convection in an Inclined Rectangular Box With the Lower Surface Half-Heated and Half-Insulated

The pattern of circulation and the rate of heat transfer were determined experimentally and also by three-dimensional, finite-difference calculations for an inclined $2 \times 1 \times 1$ rectangular enclosure with a 1×1 segment of the lower 2×1 surface at a uniform temperature, the other 1×1 segment and four side walls insulated, and the upper surface at a lower uniform temperature. As contrasted with an enclosure heated and cooled on the horizontal surfaces, a fluid motion occurs and the rate of heat transfer exceeds that for pure conduction for all temperature differences and orientations. The effects of elevation of the heated and insulated segments were investigated, as well as of inclination about the longer dimension. Despite differences in the Prandtl and Rayleigh numbers, the observed and predicted patterns of circulation are in good agreement, and the measured and predicted rates of heat are in qualitative agreement.

Introduction

Natural convection in inclined rectangular enclosures has been studied extensively in recent years owing to its application to solar collectors. In most of these investigations, the lower surface has been assumed to be at an essentially uniform temperature. However, in real solar collectors the cooling coil or jacket and the edges of the enclosure may produce a significant nonuniformity of temperature on the lower plate.

The effect of nonuniformities in the surface temperature of enclosures has received only limited attention. The most relevant work is that of Chao et al. [1], who investigated theoretically the effect of sawtooth variations in the temperature of the lower surface of $1 \times 1 \times 2$ box inclined about the longer dimension at $Ra = 6000$ and $Pr = 10$. All of the variations in surface temperature which were studied produced a stronger circulation and a higher overall Nusselt number than did a uniform temperature. A higher angle of inclination was required for transition from two roll cells with axes in the shorter horizontal dimension to a single circulation with its axis in the longer dimension. Otherwise, the pattern of circulation was unchanged.

Other work on nonuniform surface temperatures is illustrated by the following examples. Chu and Churchill [2] studied, both theoretically and experimentally, the effect of the size and location of an isothermal, horizontal strip in an otherwise insulated vertical surface of a rectangular channel. Hanzawa et al. [3] computed the velocity and temperature fields for laminar flow through a channel with a 1 to 1.2 height-to-width ratio, heated isothermally on the central half of the base with the balance of the walls at a lower uniform temperature. They predicted, and confirmed experimentally, two symmetrical roll cells superimposed on the forced flow.

Boehm and Kamyab [4] computed laminar free convection for isothermal heating of alternate, equally wide strips of a large horizontal plate facing upward in an unconfined fluid; the intermediate strips were insulated or at a lower uniform temperature. The Nusselt number for large Ra (with both dimensionless groups based on the average surface temperature and the total area) was found to be higher than for a completely isothermal surface. Torrance and coworkers [5, 6], Greenspan and Schultz [7], and others have studied the effect of a hot spot in the lower surface of an enclosure, as a simulation of a fire. None of these latter six investigations are directly relevant to natural convection in the enclosed air space of a solar collector, or to the work reported herein, owing to the fundamentally different boundary conditions.

In this study, the effect of insulating half of the lower surface was investigated as an exaggerated and presumably bounding case of the nonuniformity due to the individual cooling coils or passages of solar collectors. Three-dimensional, finite difference calculations were utilized to predict the pattern of circulation and the related rates of heat transfer. Photographs of particle paths were used to test the reliability of the computations in predicting the pattern of flow.

Three modes of inclination of the heated surface from the horizontal were investigated, as illustrated in Fig. 1. In (a) the shorter horizontal dimension is inclined about the longer dimension as an axis, in (b) the insulated end is elevated with the opposite shorter horizontal edge in the same plane as an axis, and in (c) the heated end is elevated with the corresponding opposite shorter edge as an axis. It may be noted in advance that cases (b) and (c) would not be expected to be identical or even symmetrical.

A $2 \times 1 \times 1$ enclosure was chosen for the calculations since greater aspect ratios would exceed the capability of our current computational facilities for such involved three-dimensional behavior. The results, although quantitatively applicable only for solar collectors with rectangular honey-

¹Presently Senior Staff Engineer, Mobil R&D Corporation, Paulsboro, N.J. Contributed by the Heat Transfer Division and presented at the AIAA/ASME Fluids, Plasma, Thermophysics, and Heat Transfer Conference, St. Louis, Mo., June 7-11, 1982. Manuscript received by the Heat Transfer Division June 1, 1982. Paper No. 82-HT-72.

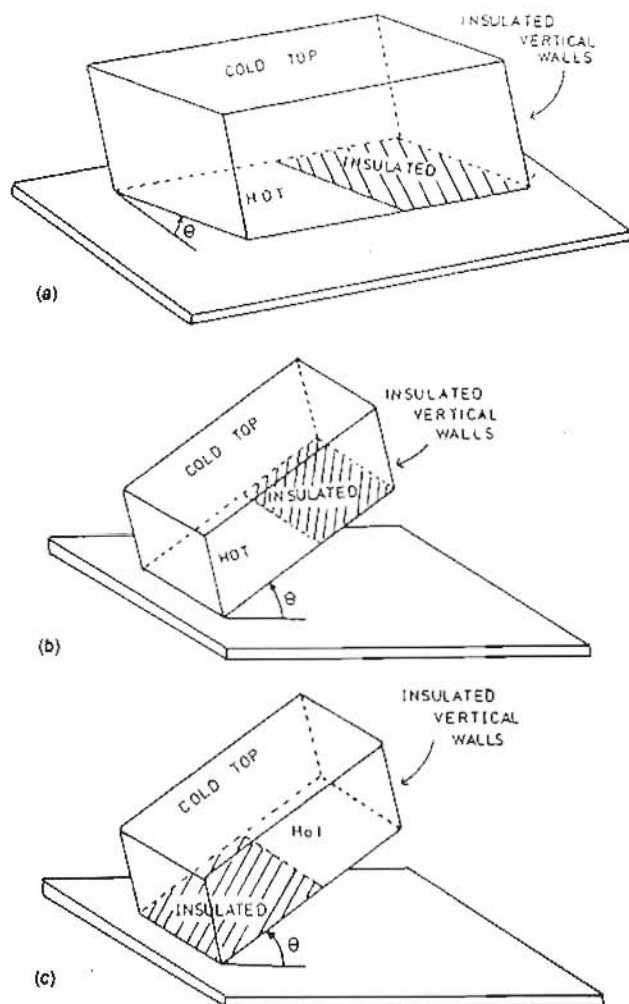


Fig. 1 Schematic drawing of different inclinations of a $2 \times 1 \times 1$ rectangular enclosure with a half-insulated and half-heated lower surface: (a) inclination of the shorter dimension; (b) elevation of the insulated end; (c) elevation of the heated end

combs, nevertheless provide qualitative information on the effect of nonuniform heating on enclosures of large aspect ratio.

Large Prandtl number fluids were used in the experimental work because of difficulties in photographing the patterns of circulation and measuring the rate of heat transfer accurately in air. Extensive experimental work by dozens of investigators (see, Churchill [8]) on natural convection in enclosures has failed to reveal a significant dependence of the Nusselt number on the Prandtl number for a Prandtl number greater

than 0.7 and a fixed Rayleigh number. In prior experimental work for rectangular enclosures, Ozoe et al. [9] found the angles of inclination for the minimum and maximum in the Nusselt number to be independent of the Prandtl number. Hence, our calculations were limited to a single Prandtl number, and the experimental fluids were chosen to optimize the experimental precision.

The necessity of a reasonable temperature difference between the heated and cooled plates established a minimum Rayleigh number of about 8000 for the measurements of heat transfer. A Rayleigh number of 25,000 proved necessary for the streakline photography. On the other hand, the maximum Rayleigh number which was feasible computationally was 10,000 for inclinations about the longer dimension as an axis, and 6000 for inclinations about the shorter dimension as an axis. These discrepancies in the range of the Rayleigh number preclude quantitative comparisons of the experimental and computation results. Fortunately, the above cited work of Ozoe et al. [9] also indicates that the qualitative dependence of the flow pattern and the Nusselt number on the Rayleigh number does not change significantly over this range.

Theoretical Model and Calculations

The calculations were for one 1×1 segment of the lower surface of the $2 \times 1 \times 1$ enclosure at a uniform, dimensionless temperature U of $+0.5$. The other 1×1 segment, as well as the four side walls, were postulated to be perfectly insulated. The upper surface was at a lower, uniform, dimensionless temperature of -0.5 .

The three-dimensional equations for the conservation of mass, energy, and momentum, as simplified by the well-known Boussinesq approximations, were postulated to describe the behavior. This model, its finite difference approximation, and the method of solution were essentially the same as that used by Ozoe et al. [10], and hence will only be outlined in this paper. The introduction of the vector potential and the vorticity permits replacement of the continuity equation and the three equations for the conservation of momentum with three equations for the conservation of vorticity. These equations were then solved in transient form together with the energy equation. The components of the vector potential were calculated from the definition of the vorticity, and the components of the velocity from the definition of the vector potential. A false transient term was added to the elliptic equation relating the vector potential and vorticity in order to obtain a parabolic form. The unknown vorticities at the wall were computed from the velocity gradients. For the numerical calculations, the derivatives in space were approximated by central differences. This scheme is not conservative, but, as previously demonstrated by Chu and Churchill [11], the resulting heat fluxes through all planes extrapolate to the same value for zero grid size. The three-dimensional, alternating-direction implicit method developed

Nomenclature

A = area of upper, cooled surface, m^2
 g = acceleration due to gravity, m/s^2
 h = grid size as fraction of H
 H = height of enclosure, m
 k = thermal conductivity, $W/m \cdot K$
 Nu = Nusselt number = $qH/kA(T_i - T_u)$
 Pr = Prandtl number = ν/α
 q = heat flux, W
 Q = dimensionless heat flux = q/q_c
 Ra = Rayleigh number = $g\beta(T_i - T_u)H^3/\nu\alpha$

T = temperature, K
 U = dimensionless temperature = $(T - 1/2T_i - 1/2T_u)/(T_i - T_u)$
 x = distance in long dimension, m
 X = dimensionless distance in long dimension = x/H
 y = distance in short horizontal dimension, m
 Y = dimensionless distance in short dimension = y/H
 z = distance from cooled plate, m
 Z = dimensionless distance from cooled plate = z/H

α = thermal diffusivity, m^2/s
 β = volumetric coefficient of expansion with temperature, K^{-1}
 ν = kinematic viscosity, m^2/s
 θ = angle of inclination of heated surface, rad

Subscripts

c = by conduction
 l = on heated surface
 u = on cooled surface

by Brian [12] was used. The matrices were solved iteratively at each time step as required for convergence. The steps in time proceeded until the steady state was closely approached.

The problem considered herein required the following two modifications: (i) the condition $\partial U/\partial Z = 0$ was substituted for $U = 0.5$ over the insulated portion of the lower surface, and (ii) as illustrated in Fig. 2, the finite difference approximation for the second derivative of U in the Z -direction along the border between the insulated and isothermal segments of the lower surface, was written as

$$\left(\frac{\partial^2 U}{\partial Z^2}\right)_{Z=0.5} = \frac{1}{2} \left[\frac{U_1 - 2U_2 + U_3}{(\Delta Z)^2} + \frac{U_2 - 2U_3 + U_4}{(\Delta Z)^2} \right] \\ = \frac{0.5U_1 - 1.5U_2 + U_3}{(\Delta Z)^2} \quad (1)$$

That is, one half of the element was taken to be isothermal at the temperature of the heated segment ($U_3 = 0.5$), while the other half was adiabatic and thus had a surface temperature equal to that of the adjacent grid point in the fluid, U_2 . This formulation was found by Chu and Churchill [11] to produce a more rapid convergence to the exact solution as the grid size was reduced, than the use of a single unknown U_3 at the edge of the insulation.

The finite difference computations were carried out on the IBM 360/175 computer of the Department of Physics of the University of Pennsylvania for $Pr = 10$, Rayleigh numbers of 4000, 6000, and 10,000, and a complete series of inclinations from 0 to π rad. This value was arbitrarily chosen for Pr since, as previously noted, the behavior is known to be unchanged for larger values and only slightly for lower values down to 0.7. These values were chosen for Ra to be above the conductive regime but within the computationally stable regime for a feasible time step. Two grid sizes were used so that the computed heat fluxes could be extrapolated to zero grid size using the Richardson-Gaunt method [13], which has been validated for natural convection by Churchill et al. [14]. These two grid sizes were uniform and equal to 0.1 and 0.2 of the shorter dimension of the enclosure. Since the truncation error of the finite difference formulation was second-order throughout, the mean heat flux for zero grid size was calculated from

$$q_{h=0} = (4q_{h=0.1} - q_{h=0.2})/3 \quad (2)$$

The indicated errors for $h = 0.1$ and $h = 0.2$ were approximately 3 and 13 percent, respectively, as compared to the results obtained by extrapolation to zero grid size.

The resulting heat fluxes for zero grid size were converted to the dimensionless form, $Q = q/q_c$, by dividing by the heat flux for pure conduction with the same boundary conditions. The Nusselt number $Nu = qH/kA\Delta T$ is herein arbitrarily based on the area of the cooled surface, and hence is less than Q .

The value of the Nusselt number for pure conduction with the same boundary conditions was found from finite difference calculations to be

$$Nu_c = \frac{q_c H}{kA\Delta T} = 0.69 \quad (3)$$

It follows from equation (3) that

$$Nu = \frac{qH}{kA\Delta T} = 0.69 Q \quad (4)$$

Streaklines were computed from the calculated velocity field for a grid size of 0.1, and the results were displayed isometrically and dynamically on a cathode ray tube, as described by Yamamoto et al. [15]. Photographs were taken of static displays. The inaccuracy due to the use of the calculations with $h = 0.1$ for the generation of these displays is sufficiently small so as to produce the qualitatively correct behavior, which is of principal interest.

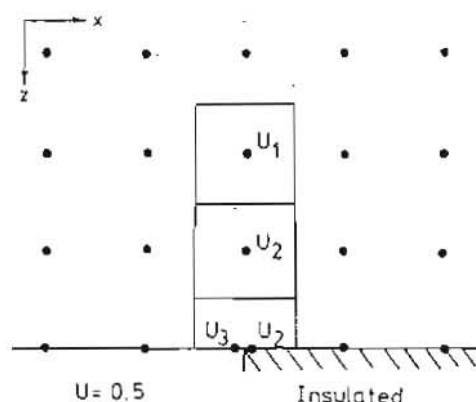


Fig. 2 Finite-difference approximation of the boundary condition at the intersection of the heated and adiabatic segments of the lower surface

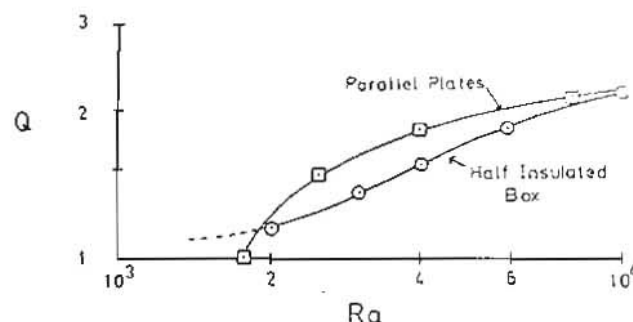


Fig. 3 Computed dimensionless heat flux in a $2 \times 1 \times 1$ rectangular enclosure with a half-heated lower surface as compared with isothermal, infinite, parallel plates

The computed steady-state results were found to be independent of the initial conditions. Hence the steady state for the previous case was usually utilized to save computing time.

Theoretical Results

Heat Transfer Rates.

No Inclination (Heating From Below). The computed, dimensionless, mean heat flux for the half-heated and half-insulated lower surface of the $2 \times 1 \times 1$ enclosure is compared in Fig. 3 with that for infinite parallel plates with isothermal upper and lower surfaces. In the later idealized case, heat transfer is by pure conduction ($Q=1$) below a Rayleigh number of 1708. For the half-insulated surface the isotherms are not horizontal even for pure conduction. Hence, natural convection occurs for all temperature differences, $Q=1$ only as $Ra=0$, and a critical Rayleigh number does not exist. It follows that Q for the half-insulated lower surface exceeds Q for infinite isothermal plates as $Ra=0$. A crossover would also occur, but at a higher Ra , for a $2 \times 1 \times 1$ enclosure with isothermal horizontal surfaces. If the results were plotted in terms of Nu (based on the cooled area) instead of Q , a crossover would not occur, since in this form the doubled area for heating with an isothermal surface overcomes the finite convection with half-heating, even for $Ra=0$.

Inclination of the Shorter Horizontal Dimension About the Longer Dimension as an Axis. The mean Nusselt number for the cooled surface is plotted in Fig. 4 for a complete range of inclinations of the half-insulated surface from the horizontal and for Rayleigh numbers of 4000, 6000, and 10,000. Nu is seen to go through a minimum at about $2\pi/180$ to $5\pi/180$ rad and a maximum at about $45\pi/180$ rad, and then to decrease to a value slightly above 0.7 at π rad, corresponding to heating from above. Because of the unsymmetrical heating, some convection occurs even in the

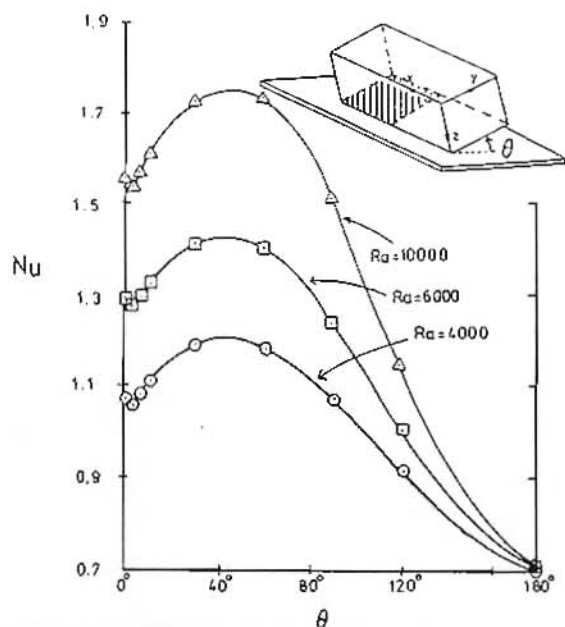


Fig. 4 Predicted mean Nusselt number for inclination of the shorter horizontal dimension (about the longer horizontal dimension as an axis) of a $2 \times 1 \times 1$ rectangular enclosure with a half-heated lower surface

latter limit. The minimum is attributed to the transition from one mode of circulation to another, as described below.

For a uniform temperature on the lower surface, the mean Nusselt number, as computed by Ozoe et al. [16], varies similarly with the angle of inclination but is approximately one-third higher.

Elevation of the Unheated End of the Enclosure About the Shorter Horizontal Dimension as an Axis. The behavior for this case, as illustrated in Fig. 5, is qualitatively similar to that for inclination about the longer dimensions as an axis. However, the minimum occurs at about $5\pi/180$ rad and the maximum at about $60\pi/180$ rad. The latter value is in close agreement with the prediction of $63.4\pi/180$ rad by Churchill and Ozoe [17]. Again, the minimum is associated with a transition in the mode of circulation, as described below.

Elevation of the Heated End About the Shorter Horizontal Dimension as an Axis. As illustrated in Fig. 6, a minimum does not occur for this case. This result is consistent with the absence of a transition in the mode of circulation, as discussed below. The maximum occurs at the somewhat lower angle of about $50\pi/180$ rad.

Streaklines.

Photographs were taken of static displays of the computed streaklines for $Ra = 6000$ and various inclinations on the cathode ray tube of the Vector General 3404 Graphic Display Unit of the Computer Graphics Laboratory of the School of Engineering and Applied Science of the University of Pennsylvania. Dynamic displays of the streaklines were used to determine the direction and speed of circulation.

Elevation of the Shorter Horizontal Dimension About the Longer Dimension as an Axis. Perspective views of the streaklines as photographed from the cathode ray tube are shown in Fig. 7 for inclination about the longer dimension as an axis (as in Fig. 4). Different viewing angles (not to be confused with the angle of elevation of the enclosure) were used to better elucidate the fluid motion. The heated segment is at $Z = 1$ (bottom) and $0 \leq X \leq 1$. The Y -axis is inclined.

For no inclination, as shown in Fig. 7(a) and somewhat better in Fig. 8(a), the motion consists of two symmetrical roll-cells with a 2×1 cross section. These roll-cells have a

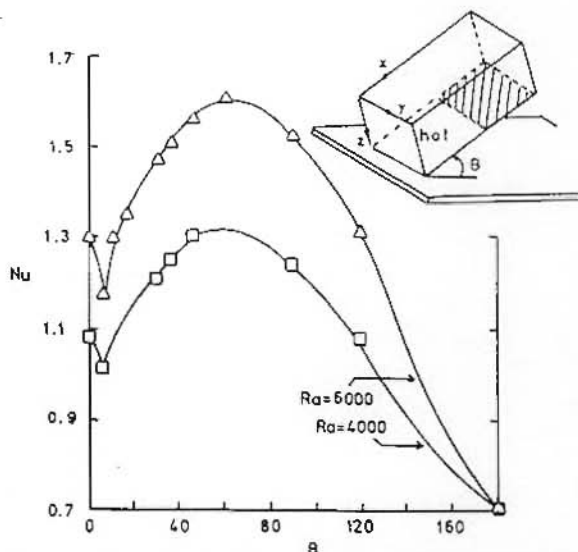


Fig. 5 Predicted mean Nusselt number for elevation of the unheated end (about the shorter horizontal dimension as an axis) of a $2 \times 1 \times 1$ rectangular enclosure with a half-heated lower surface

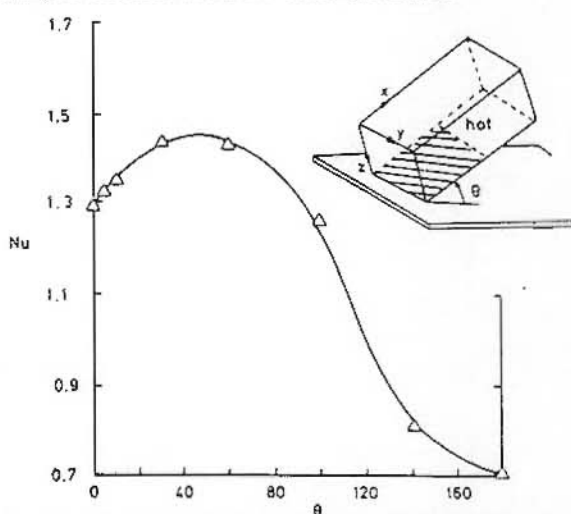


Fig. 6 Predicted mean Nusselt number at $Ra = 6000$ for elevation of the heated end (about the shorter horizontal dimension as an axis) of a $2 \times 1 \times 1$ rectangular enclosure with a half-heated lower surface

common axis and could be considered to be a single gross roll-cell except that they do not interchange fluid. Their axes are parallel to the shorter dimension (Y -axis) and displaced somewhat from the midplane ($X = 1$) toward the heated end. From the dynamic display, the motion was observed to be upward at the heated end of the enclosure, along the upper, cooled surface ($Z = 0$), downward at the insulated end, and back along the insulated segment ($X > 1$) of the lower ($Z = 1$) surface.

As the enclosure is inclined about the longer dimension, the two roll-cells become increasingly oblique, distorted, and dissimilar, as illustrated in Figs. 7(b), (c), (d) for $2\pi/180$, $6\pi/180$ and $10\pi/180$ rad, respectively. They retain a common but highly curved axis. For an inclination greater than $10\pi/180$ rad, the plane of separation between the two roll-cells crosses the diagonal plane between the vertical edges of the enclosure, and a gradual transition occurs. Following the transition, the roll-cells are relocated in the left and right hands of the enclosure, as illustrated in Figs. 7(e) and (f) for $60\pi/180$ and $90\pi/180$ rad, respectively. The portion of the common axis associated with the left hand roll-cell is now nearly parallel to the longer dimensions of the enclosure, but that of the right-hand roll-cell is somewhat oblique.

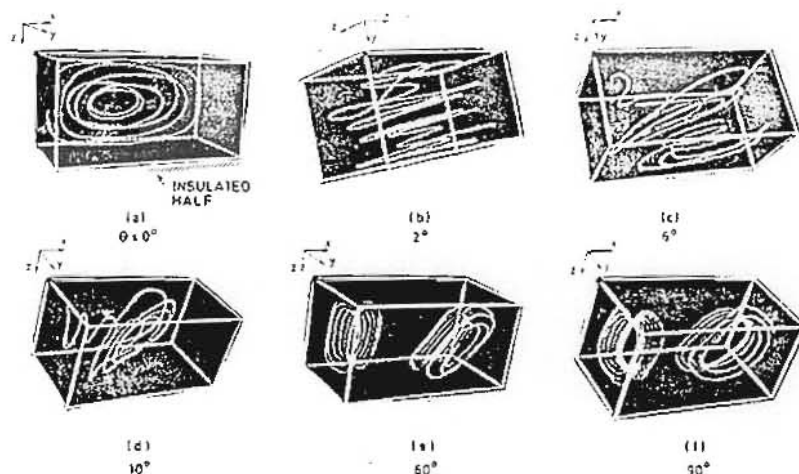


Fig. 7 Perspective view of computed streaklines at $Ra = 6000$ for inclination of the shorter horizontal dimension (about the longer dimension as an axis) of a $2 \times 1 \times 1$ rectangular enclosure with a half-heated lower surface (heated surface is at $Z = 1$, $X < 1$; angle θ is between the horizontal plane and the X - Y -plane)

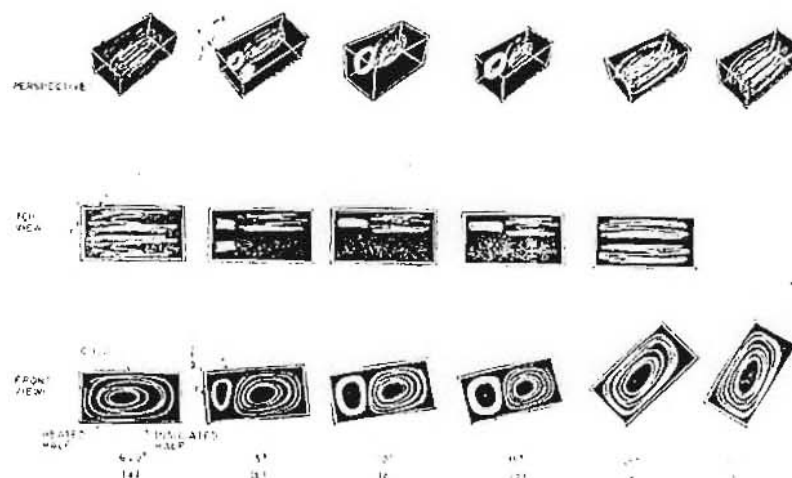


Fig. 8 Perspective, top and front views of computed streaklines at $Ra = 6000$ for elevation of the unheated end of a $2 \times 1 \times 1$ rectangular enclosure with a half-heated lower surface

This behavior contrasts with that described by Ozoe et al. [16] for a $2 \times 1 \times 1$ box with a uniform surface temperature. In the latter case, the stable motion for a horizontal orientation consists of four roll-cells with 1×1 cross sections, and again with axes parallel to the shorter horizontal dimension. These cells are symmetrical with respect to the two vertical midplanes of the enclosures but the direction of circulation of the pair of cells at each end is up along the 1×1 end walls and down along the midplane, or the reverse, depending on the initial conditions. Upon inclination about the longer dimension, the four roll-cells retain their integrity, and their symmetry with respect to the 1×1 vertical midplane, but become increasingly distorted and unsymmetrical with respect to the 2×1 vertical midplane. At an inclination of about $2\pi/180$ rad the plane of separation of the two roll-cells at either end of the enclosure crosses the diagonal plane of that half of the enclosure and a transition of each pair of roll-cells to a single roll-cell with its axis exactly parallel to the longer dimension occurs. The two consolidated roll-cells have a common axis parallel to the longer dimension of the enclosure, and, as contrasted with the half-heated case, are perfectly symmetrical with respect to the vertical 1×1 midplane of the enclosure.

Elevation of the Unheated End About the Shorter Horizontal Dimension as an Axis. Photographs for the cathode ray tube of perspective, top and front views are shown in Fig. 8 for several elevations of the unheated end of the enclosure (as in Fig. 5). For this type of elevation, symmetry is maintained with respect to the vertical 2×1 midplane. For very small inclinations the two roll-cells of Figs. 7(a) and 8(a) persist although their common rate of circulation decreases. At an inclination of less than $5\pi/180$ rad two new, small roll-cells are generated at the heated end. These new roll-cells circulate up along the inclined heated surface in correspondence to the buoyant force. Due to the elevation of the unheated end, the circulation of the original roll-cells is in opposition to the buoyant force. Initially, this reverse circulation is maintained by induction from the new roll-cells, but as the inclination is further increased, the new roll-cells grow in size and strength at the expense of the original ones, and the latter eventually vanish, resulting in, as indicated in Fig. 8(d) and (e), a circulation similar to that for no inclination, but in the opposite direction. The minimum in the rate of heat transfer, as shown in Fig. 5, appears to correspond to the appearance of the two new roll-cells.

For a uniform temperature on the lower surface, whichever

pair of roll-cells is circulating in correspondence to the buoyant force grows at the expense of the other pair, the second pair disappearing at an inclination of about $10\pi/180$ rad (see again, Ozoe et al. [16]).

Elevation of the Heated End About the Shorter Horizontal Dimension as an Axis. When the heated end of the enclosure is elevated, the strength of the circulation increases and then decreases, but the mode does not change from that of Figs. 7(a) and 8(a), since the direction of circulation of the long roll-cells for no inclination is already in correspondence with the buoyant force for an inclined enclosure. The behavior for a uniform temperature on the lower surface is independent of the elevated end and hence is as described in the previous paragraph.

Photography of Flow Patterns

Apparatus.

Photographs of experimental flow patterns were taken at Okayama University in an enclosure with internal dimensions of $31 \times 31 \times 62$ mm. The upper plate and half of the lower plate were of 10-mm thick copper, resulting in a negligible variation in temperature. The four side walls and the insulated half of the lower plate were plexiglass, also 10-mm thick. The upper plate was cooled by circulating water from a 301 ± 0.1 K bath through a jacket. The lower copper plate was heated similarly by circulating water from a constant (but higher) temperature bath, but the heating was changed to electric resistance during the flow visualization experiments. The entire apparatus was covered with glass-fiber insulation (except when taking photographs) and the room was maintained at the temperature of the cooling water to minimize heat exchange with the surroundings. The temperature difference between the upper and lower copper plates was measured with embedded copper-constantan thermocouples.

Two small holes for tracer injection were drilled at the middle height at 15.5 mm from the ends of the enclosure. Vinyl tubes were inserted into these holes and a syringe was used to inject the tracer.

Conditions.

The working fluid was glycerol. The Rayleigh number was established at approximately 25,000 (with a plate-temperature difference of ~ 4 K) for each inclination, since this was the lowest value for which it was possible to obtain good photographs without anomalous dispersion of the tracer particles. On the other hand, finite difference calculations were not feasible for such a high Rayleigh number, owing to an inordinate restriction on the time steps. As noted above, prior results for a uniform temperature on the lower surface indicate that this difference in Rayleigh number would not be expected to change the circulation pattern even though the rates of circulation and heat transfer differ considerably. The difference in Prandtl number would be expected to change the rate of circulation but not the pattern.

Ten hours or more were allowed for the enclosure to reach hydrodynamic and thermal equilibrium. A variation of less than $0.1 \mu\text{V}$, equivalent to 0.0024K , in the thermocouple readings over the copper plates was used as a further criterion of the attainment of a steady state. (In all cases a unique and nonoscillatory state was observed.) Thereafter, 0.5 ml of a dense dispersion of aluminum particles in glycerol was injected into the enclosure through each of the two holes at a depth of 3 mm. Forty to ninety minutes later, the insulation was removed to permit photographing the traces of these particles. Photographs were taken from both the long and the short sides with $\pi/2$ rad illumination of the whole surface from a projector lamp. ASA 400 black and white film was used with a Nikon f2 Photomic camera having an f3.5 Micro Nikkor lens, at a setting of f11 and an exposure time of 15 s.

Photographic Results

Elevation of Unheated End About the Shorter Dimension as an Axis. Photographs of the aluminum particles for elevation of the right (unheated) end are shown in Fig. 9. These side and front views reveal a circulation pattern in qualitative agreement with the computed streaklines of Fig. 8, despite the higher Rayleigh number. A minor discrepancy is the failure of the new, reversely circulating roll-cells to appear experimentally until the inclination exceeded $5\pi/180$ rad.

Elevation of Shorter Horizontal Dimension About the Longer Dimension as an Axis. Similar photographs for elevation of the shorter dimension are shown in Fig. 10. Again, the results are consistent with the computed streaklines of Fig. 7 for similar conditions.

Experimental Heat Flux Measurements

Apparatus and Operation. The same enclosure and operating conditions were used for the heat flux measurements as for the photographs of particle paths, except that the maintenance of the same surface temperature at different elevations was found to be easier when hot circulating water was used for heating, rather than electricity. The heat flux was measured by placing a heat-flux meter pad over the heated segment. The surface-temperature was measured by a single thermocouple integral with and at the center of the pad. The temperature variation over the heated and cooled copper surfaces was completely negligible owing to their 10-mm thickness, but the surface temperature of the pad was slightly lower. Silicone oil with $\text{Pr} \approx 3200$ was used as the working fluid. Runs were carried out at $\text{Ra} = 7790$ and



Fig. 9 Photographs of aluminum particles in glycerol at $\text{Ra} = 25,000$ in a $62 \times 31 \times 31$ -mm rectangular enclosure with elevation of the unheated end of the half-heated lower surface



Fig. 10 Photographs of aluminum particles in glycerol at $Ra = 25,000$ in a $62 \times 31 \times 31$ -mm rectangular enclosure with inclination of the shorter dimension of the half-heated lower surface

13,300. The silicone oil was chosen because of the relatively small variation in its viscosity with temperature. As noted above, the choice of Rayleigh numbers extending upward from the computed range followed from the necessity of a reasonable temperature difference between the plates. Even then, the small temperature differences of 1–2 K precluded the establishment of precise, prechosen values of the Rayleigh number.

Results. The experimentally determined Nusselt numbers for elevation of the unheated end about the shorter horizontal dimension as an axis are compared with the computed values in Fig. 11. The predicted maximum at about $45\pi/180$ rad and minimum at about 2 to $5\pi/180$ rad are both observed. Good qualitative agreement can also be observed between the predictions for $Ra = 6000$ and $Pr = 10$, and the measurements for $Ra = 7790$ and $13,300$ and $Pr = 3130$ – 3170 for elevations greater than $\pi/6$ rad. The experimental Nusselt numbers for lesser inclinations fall far below the predicted values.

Figure 12 is a similar comparison for elevation of the heated end about the shorter horizontal dimension as an axis. In this case, the measurements confirm the predictions qualitatively, with a maximum at about $45\pi/180$ rad and no minimum, but are much lower at all angles.

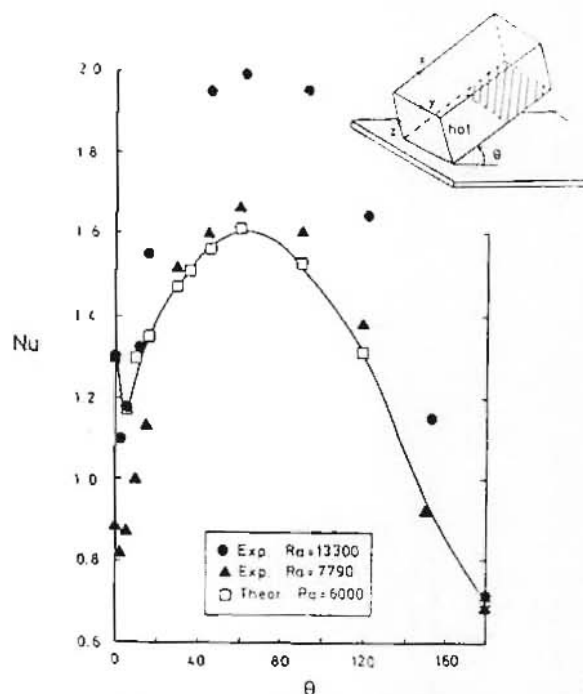


Fig. 11 Comparison of experimental and predicted mean Nusselt numbers for elevation of the unheated end of the half-heated lower surface of a $2 \times 1 \times 1$ rectangular enclosure

● Experimental, $Ra = 13300$, $Pr = 3130$
 ▲ Experimental, $Ra = 7790$, $Pr = 3170$
 □ Theoretical, $Ra = 6000$, $Pr = 10$

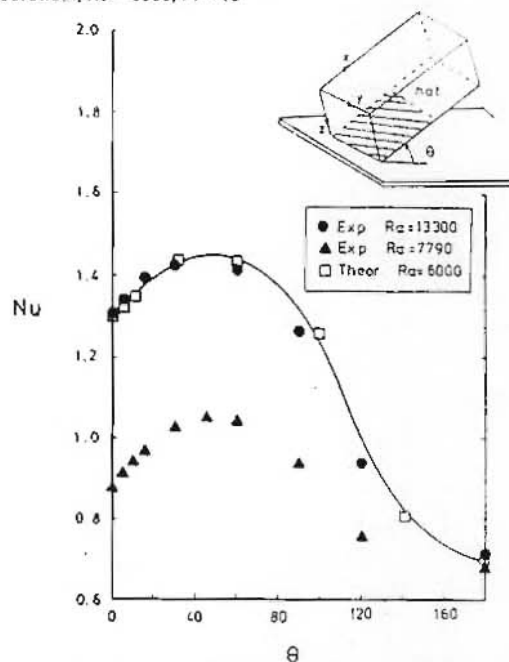


Fig. 12 Comparison of experimental and predicted mean Nusselt numbers for elevation of the heated end of the half-heated lower surface of a $2 \times 1 \times 1$ rectangular enclosure

The foregoing discrepancies are presumed to be due to heat flow along and through the plexiglass section of the lower plate. For elevation of the heated end, this unaccounted heat flow generates a pair of secondary roll-cells with reverse circulation, thereby impeding the pair of primary roll-cells and decreasing the overall rate of convection between the uninsulated half of the high-temperature surface and the cooled surface. As noted previously, the theoretical calculations for perfect insulation do not produce a pair of

secondary roll-cells for elevation of the heated end.

In the case of elevation of the unheated end, heat flow through the plexiglass apparently tends to impede the motion of the original roll-cells above the insulation (as shown on the right-hand side of Fig. 8(b), (c), and (d), and on the right-hand side of the front view in Fig. 9(c), (d), and (e)), thereby decreasing the overall rate of convection. After the original roll-cells vanish, at elevations above $35\pi/180$ rad, the effect of the heat flow through the plexiglass is apparently less important.

Conclusions

Insulating a portion of the heated surface of an inclined rectangular enclosure produces significant changes in the mode of circulation and rate of heat transfer relative to a completely isothermal surface. These changes may be of practical importance in solar collectors and in space heating.

The asymmetry due to insulating half of the heated surface results in circulation for all temperature differences and orientations. Thus, there is no critical Rayleigh number for heating from below, and the rate of heat transfer always exceeds that for pure conduction with the same boundary conditions. Some circulation and a rate of heat transfer exceeding that for pure conduction with the same boundary conditions also occur for heating from above. However, the absolute rate of heat transfer with a uniform temperature on the lower plate still exceeds that for half-heating at all inclinations and for all of the Rayleigh numbers which were investigated, primarily because the heated (lower) area is twice as big.

If the Nusselt number were based on the heated area rather than on the cooled area, it would exceed that for surfaces with uniform temperatures for all conditions. This result is in accord with the conclusion reached by Chao et al. [1] that surface temperature variations produce higher heat transfer rates than do uniform temperatures.

The number of roll cells appears to be associated with the area of heating rather than with the total area. Thus, one pair of roll-cells occurred for heating of half of the lower surface as compared to two pairs of roll-cells for uniform heating.

Photographs of particle paths were in good agreement with computed streaklines despite differences in the Rayleigh and Prandtl numbers, thus providing confidence in the computed rates of heat transfer.

Streaklines were found to be invaluable in interpreting the behavior. For example, the variation of the mean Nusselt number with the type and degree of inclination can be explained directly in terms of the changes in strength and mode of the circulation pattern. Specifically, the minimum in the Nusselt number is observed to occur in conjunction with the change in the mode of circulation for elevation of the shorter dimension or the insulated end of the enclosure, whereas no minimum and no change of mode occur for elevation of the heated end at angles greater than $30\pi/180$ rad about the shorter horizontal dimension as an axis. For lesser elevations of the heated end and for elevations of the unheated end the

The experimentally measured heat fluxes are in qualitative agreement with the computed values for elevation of the heated end at angles greater than $30\pi/180$ rad about the shorter horizontal dimension as an axis. For lesser elevations of the heated end and for elevations of the unheated end the experimental values follow the same trends as the predictions but fall significantly lower for the same Ra. This discrepancy is attributed to finite conduction along and through the plexiglass plate comprising the insulated half of the initially lower plate, resulting in a small counter-circulation.

The theoretical results of this investigation and of Chao et al. [1], as well as the above experimental discrepancies, in-

dicate that unintentional and undocumented deviations from isothermality and/or perfect insulation may produce significant and anomalous effects. This failure to simulate the nominal boundary conditions is undoubtedly responsible in large part for the well-known scatter and discrepancies in experimental measurements of natural convection in enclosures. (Such effects should not be confused with the significant error involved in most experimental determinations of the heat flux within the fluid.)

Acknowledgment

This work was supported in part by the U.S. Department of Energy, Solar Heating and Cooling R&D Branch, through contract EM-78-04-5365, and in part by Special Projects on Energy Problems, of Grants in Aid for Scientific Research, the Ministry of Education, Japan (No. 57040075). The participation of Professor Ozoe in the work at University of Pennsylvania was cosponsored by the Japan Society for the Promotion of Science and the U.S. National Science Foundation.

The assistance of Akira Yamamoto, Ikuo Shida, Akira Mouri, and Shozo Mishima of Okayama University is gratefully acknowledged.

References

- 1 Chao, P. K.-B., Ozoe, H., and Churchill, S. W., "The Effect of a Non-Uniform Surface Temperature on Laminar Natural Convection in a Rectangular Enclosure," *Chem. Eng. Commun.*, Vol. 9, 1981, pp. 245-254.
- 2 Chu, H. H.-S., and Churchill, S. W., "The Effect of Heater Size, Location, Aspect Ratio and Boundary Conditions on Two-Dimensional, Laminar Natural Convection in Rectangular Channel," *ASME JOURNAL OF HEAT TRANSFER*, Vol. 98, 1976, pp. 194-201.
- 3 Hanzawa, T., Ito, U., and Tadaki, T., "Heat Transfer by Natural Convection in an Enclosed Cavity—A Part of the Bottom is Heated," (in Japanese) *Kagaku Kogaku Ronbunshu*, Vol. 1, 1975, pp. 450-453.
- 4 Boehm, R. F., and Kamyab, D., "Established Stripwise Laminar Natural Convection on a Horizontal Surface," *ASME JOURNAL OF HEAT TRANSFER*, Vol. 99, 1977, pp. 294-299.
- 5 Torrance, K. E., Orloff, L., and Rockett, J. A., "Experiments on Natural Convection in Enclosures With Local Heating from Below," *Journal of Fluid Mech.*, Vol. 36, 1969, pp. 21-31.
- 6 Torrance, K. E., and Rockett, J. A., "Numerical Study of Natural Convection in an Enclosure With Localized Heat From Below—Creeping Flow to the Onset of Laminar Instability," *Journal of Fluid Mech.*, Vol. 36, 1969, pp. 33-54.
- 7 Greenspan, D., and Schultz, D., "Natural Convection in an Enclosure With Localized Heating from Below," *Computer Methods Appl. Mechanics and Engineering*, Vol. 3, 1974, pp. 1-10.
- 8 Churchill, S. W., "Free Convection in Layers and Enclosures," *Heat Exchanger Design Handbook*, ch. 2.5.8, edited E. U. Schlunder, Hemisphere Publishing, Washington, D.C., 1983.
- 9 Ozoe, H., Sayama, H., and Churchill, S. W., "Natural Convection in an Inclined Rectangular Channel at Various Aspect Ratios and Angles—Experimental Measurements," *International Journal of Heat and Mass Transfer*, Vol. 18, 1975, pp. 1425-1431.
- 10 Ozoe, H., Yamamoto, K., Churchill, S. W., and Sayama, H., "Three-Dimensional, Numerical Analysis of Laminar Natural Convection in a Confined Fluid Heated From Below," *ASME JOURNAL OF HEAT TRANSFER*, Vol. 98, 1976, pp. 202-207.
- 11 Chu, H. H.-S., and Churchill, S. W., "The Development and Testing of a Numerical Method for Computation of Laminar Natural Convection in Enclosures," *Computers and Chem. Engrg.*, Vol. 1, 1977, pp. 103-108.
- 12 Brian, P. L. T., "A Finite Difference Method of High-Order Accuracy for the Solution of Three-Dimensional Transient Heat Conduction," *AIChE Journal*, Vol. 7, 1961, pp. 367-370.
- 13 Richardson, L. F., and Gaunt, J. A., "The Deferred Approach to the Limit," *Phil. Trans. Roy. Soc., London, Ser. A*, Vol. 226, 1972, pp. 299-361.
- 14 Churchill, S. W., Chao, P., and Ozoe, H., "Extrapolation of Finite-Difference Calculations of Laminar Natural Convection in Enclosures to Zero Grid-Size," *Num. Heat Transfer*, Vol. 4, 1981, pp. 39-51.
- 15 Yamamoto, K., Ozoe, H., Chao, P., and Churchill, S. W., "The Computation and Dynamic Display of Three-Dimensional Streaklines for Natural Convection in Enclosures," *Computers and Chem. Engrg.*, Vol. 6, 1982, pp. 161-167.
- 16 Ozoe, H., Churchill, S. W., Okamoto, T., and Sayama, H., "Three-Dimensional Natural Convection in Inclined Rectangular Enclosures," *Proc. PACHEC '77*, Vol. 1, 1977, pp. 24-31, AIChE, New York.
- 17 Churchill, S. W., and Ozoe, H., "Correlating Equations for Natural Convection in Enclosures," in preparation.